Chinese Chemical Letters 33 (2022) 2937–2941

Contents lists available at ScienceDirect

Chinese Chemical Letters

journal homepage: www.elsevier.com/locate/cclet

Nanoplateletsomes for rapid hemostasis performance

Honglan Wang[a,b,1], Yuefei Zhu[a,c,1], Longlong Zhang[a], Huiwen Liu[b], Chunying Liu[a], Bo Zhang[b], Yanan Song[a], Yu Hu[b,*], Zhiqing Pang[a,*]

[a] Key Laboratory of Smart Drug Delivery, Ministry of Education, School of Pharmacy, Fudan University, Shanghai 201203, China
[b] Institute of Hematology, Union Hospital, Tongji Medical College, Huazhong University of Science & Technology, Wuhan 430022, China
[c] Department of Biomedical Engineering, Columbia University, New York, NY 10027, United States

ARTICLE INFO

Article history:
Received 29 August 2021
Revised 29 December 2021
Accepted 31 December 2021
Available online 7 January 2022

Keywords:
Hemostasis
Platelets
Biomimetic
Hemorrhage
Thrombus targeting

ABSTRACT

Uncontrollable hemorrhage remains staple trouble in surgical procedures and a leading cause after major trauma. The bleeding issue may trigger various pathologic scenarios that can lead to tissue morbidities and mortalities, and currently available on-site hemostatic agents are confined to a narrow therapeutic index and may carry the risk of immunogenicity. Inspired by the crucial role of platelets in the process of thrombus, a platelet-mimetic plateletsome with wound targeting and blood coagulation properties is developed for hemorrhage control. Plateletsome is formulated by integrating platelet membranes with functionalized synthetic liposomes and exhibits superior wound targeting and effective hemostasis properties. It presents less blood loss and shorter hemostasis time than the platelet membrane vehicles or the conventional liposomes in the mouse tail transection model. The strong homing of the biomimetic plateletsome to the thrombus was also confirmed, demonstrating the potential of this engineered cell membrane vesicle as a biomimetic hemostat for bleeding treatment.

Uncontrollable hemorrhage, a serious medical emergency, is the leading cause of morbidity and mortality in traumatic and surgical injuries [1,2]. Approximately 80% of deaths were aroused from massive hemorrhage *via* penetrating and truncal bleeding in accidents or military operations [3]. Since most deaths occur during the first-time phase of bleeding complications, patients often demand coordinated, timely therapy to treat the bleeding befittingly. Recent decades have witnessed the surge of various biomaterials designed for on-site interventions such as tourniquets and topical hemostatic dressings [4,5]. Nevertheless, for internal, diffuse, and non-compressible bleeding, in addition to a few hemostatic agents [6], transfusion of blood products (*e.g.*, packed erythrocytes, fresh frozen platelets) and coagulation factor concentrates remain the mainstay clinical option for stanching hemorrhage [7]. Owing to the stern challenge of massive hemorrhage and high blood pressure aroused by the artery, trunk, and cavity hemorrhage, available drugs with lower absorption, weaker tissue adhesion, and slower activation could hardly meet these demands [8].

It is noteworthy that platelets play a profound physiological role in hemostasis regulation, protecting the body against minor and life-threatening bleeding, and sticking up for the vascular system [9,10]. Specifically, these small anucleate blood cells play a crucial part in the formation of a primary hemostatic plug through the interaction with fibrin to seal the ruptured vessels and further avert excessive blood loss upon vessel injury [11,12]. Furthermore, the platelet membrane possesses many receptors, such as GPVI, GPIb-V-IX, 5HT2A, a2A, TP, protease-activated receptors (PARs), P2Y1, P2Y12, and integrins, among others [13–15]. The multitude of platelet functions derives from a distinct set of surface moieties responsible for immune evasion [16,17], subendothelium adhesion [18], and pathogen interactions [19,20]. However, fresh frozen platelets, as one of the typical transfusion of blood products, have limitations such as short shelf life (around 5–7 days) with strict storage stipulations, considerable prescreening to avoid immunogenicity issues, as well as the potential risk of biological contamination [21,22].

Accordingly, these years, attempts have been made to mimic certain aspects of platelet-related vascular targeting [23–27]. Earlier studies have reported that nanovehicles such as liposomes were leveraged to be functionalized with fibrinogen or fibrinogen-derived peptide ligands [28]. Since liposomes are phospholipid vesicles composed of single or multiple concentric lipid bilayers enclosing aqueous spaces [29], such resulting liposomes with their biocompatible and biodegradable nature have received intense research interest. However, these methods markedly deviate from

* Corresponding authors.
E-mail addresses: dr_huyu@126.com (Y. Hu), zqpang@fudan.edu.cn (Z. Pang).
[1] These authors contributed equally to this work.

https://doi.org/10.1016/j.cclet.2021.12.091
1001-8417/

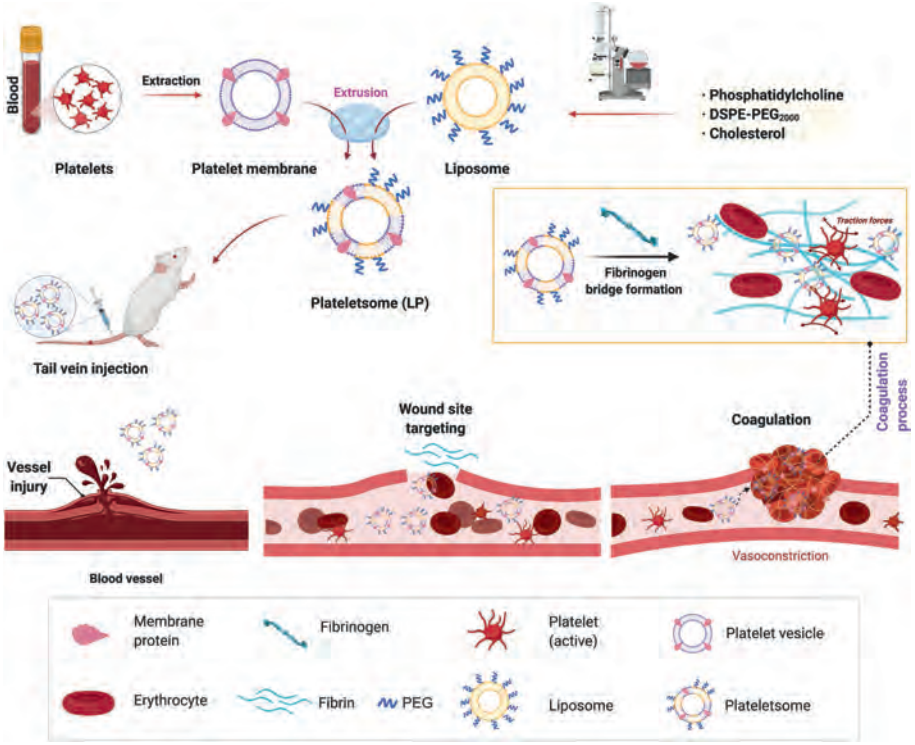

Scheme 1. Schematic illustration on the preparation of LP and the underlying hemostasis process enhanced by the LP.

the criteria by which natural platelets function in two main ways. These nanovehicles do not mimic the intricate biochemical interactions that occur when natural platelets interplay with and bind to the endothelium. On the flip side, liposomes and other polymer nanoparticles do not mimic the biophysical disk-like structure or the flexibility of natural platelets, which are essential for facilitating hemodynamic transport and efficient selective binding of platelets to the edges of endothelial cells at the site of injury [30].

In this regard, our work leverages the intrinsic hemostatic capability of platelets to constitute a hybrid nano-hemostatic agent, plateletsome, to halt the bleeding. We hypothesized that plateletsomes (LP), liposomes hybridized with platelet membranes, could combine the homing and hemostasis ability of platelets and the superior physicochemical stability of the synthetic liposomes, thus forming a nanoplatform for rapid hemostasis performance (Scheme 1). By adopting the cell membrane heterozygous technique, we demonstrate that LP conforms to the biophysical design criteria of platelet-mimetic morphology and flexibility, and exhibits the ability to target an injured vascular site to render hemostasis. Besides, their surfaces preserve the natural structures of platelet membranes, making them a distinct class of biomimetic materials that combine both natural and synthetic components. The hemostatic efficacy of LP was studied both *in vitro* and *in vivo*, and specific coagulation mechanisms were discussed from the overall body level to the protein level. The feasibility of our bioinspired nanodesign to achieve the enhanced hemostatic effect without systemic toxicity is validated. In general, it is the first time to develop an efficient and safe biomimetic hemostatic nanotherapeutics without any drug loading, which can target injured blood vessels and control massive bleeding.

In the current study, LP was synthesized through the membrane fusion of lipid membranes and PLT membranes, as illustrated in Scheme 1. The fusion study was first verified by confocal fluorescent microscopy imaging. As shown in Fig. 1A and Fig. S1 (Supporting information), liposomes (Lip) and platelet membranes (PV)

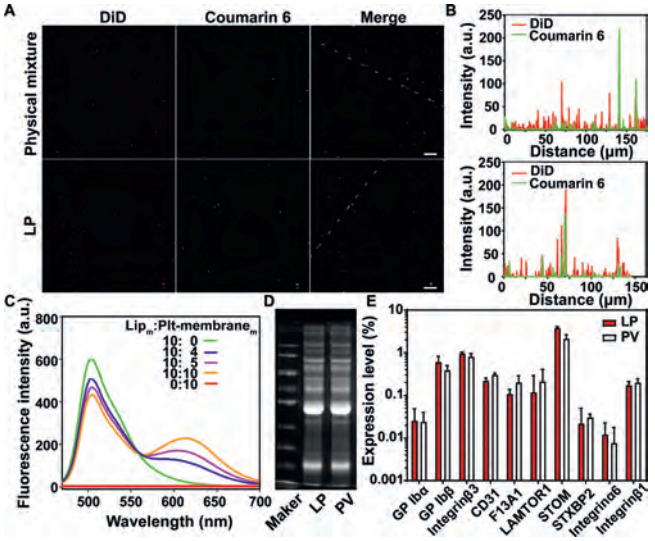

Fig. 1. Verification of LP preparation. (A) Fluorescence images of the physical mixture of liposomes and platelet membranes (up) and the LP (down) (Scale bar = 2 μm) and (B) the corresponding fluorescence intensity profiles along the dotted white line crossing the representative image. (C) The fluorescence spectra of LP with different mass ratios of lipid membranes to platelet membrane proteins. Rhodamine B-stained platelet membranes and coumarin 6-stained lipid membranes were fused to generate LP. Lip_m:Plt-$membrane_m$ indicates the mass ratio of lipid membranes to platelet membrane proteins. (D) Sodium dodecyl sulfate-polyacrylamide gel electrophoresis (SDS-PAGE) analysis of the membrane proteins in LP and PV. (E) The relative expression levels of typical membrane proteins in LP and PV were analyzed by label-free quantification proteomics technology ($n = 3$).

were labeled with fluorescent dyes coumarin 6 and DiD, respectively. There were few green fluorescence and red fluorescence signals overlap in the mixture of Lip and PV (Fig. 1B). In contrast, the significant colocalization of two fluorescent signals was observed

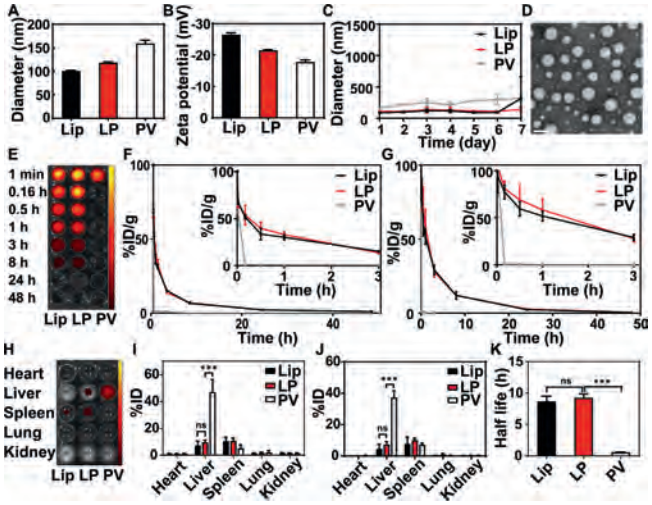

Fig. 2. Characterization of LP. (A) Diameter and (B) zeta potential of the obtained Lip, LP and PV ($n = 3$). (C) Size stability of Lip, LP and PV over 7 days in 10% FBS at 4 °C ($n = 3$). (D) Transmission electron microscopy (TEM) of LP (scale bar = 100 nm). (E) Fluorescence imaging of the blood at different time points after nanovesicle injection and (F) the corresponding semi-quantitative fluorescence intensity of the blood was plotted with the time ($n = 3$). (G) The quantitative pharmacokinetic profiles of Lip, LP and PV ($n = 5$). (H) Fluorescence imaging of the homogeneous solution of major organs at 48 h after nanovesicle injection and (I) the corresponding semi-quantitative fluorescence intensity in major organs ($n = 3$). (J) The quantitative analysis of the biodistribution of Lip, LP and PV ($n = 3$). (K) The half-life of Lip, LP and PV in the blood determined from (G) ($n = 5$). $^{***}P < 0.001$. The abbreviation "ns" indicates no significance between the two groups.

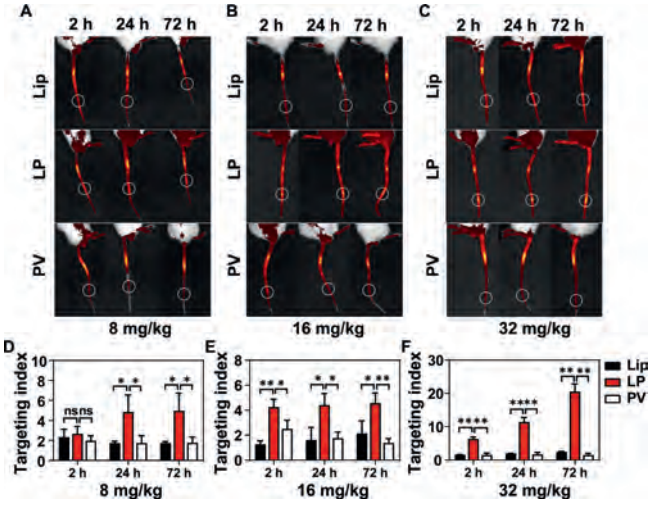

Fig. 3. *In vivo* targeting capability of LP to injury vessels ($n = 3$). Fluorescence imaging of the tails of mouse models at 2, 24 and 72 h after LP injection at the doses of (A) 8 mg/kg, (B) 16 mg/kg, and (C) 32 mg/kg. White circles indicate the injured vessels. The targeting index of different formulations at the dose of (D) 8 mg/kg, (E) 16 mg/kg, and (F) 32 mg/kg. $^{*}P < 0.05$, $^{**}P < 0.01$. The abbreviation "ns" indicates no significance between two groups.

after fusion. Afterward, the fusion of platelet membranes and artificial liposomes was further validated by FRET. As the amount of PV increased, the fluorescence intensity at 620 nm was increased while the fluorescence intensity at 510 nm decreased, suggesting the interspersing of PV in the lipid bilayer of Lip, triggering the FRET interactions in the Lip (Fig. 1C). When LP was prepared at the lipid:PLT membrane protein mass ratio of 10:1, the FRET efficiency was about 30.6%. A pull-down experiment was performed to validate the fusion of PLT membranes and lipid membranes. Coumarin 6-labeled lipid membranes functionalized with biotin-PEG-DSPE were fused with PLT membrane to form coumarin 6-labeled LP. Then LP was pulled down by the streptavidin magnetic beads. As shown in Fig. S2 (Supporting information), around 85% LP was pulled down by the beads, indicating that the Lip was not coated by the platelet membrane but fused with the platelet membrane. SDS-PAGE analysis of LP and PV demonstrated that both LP and PV exhibited the same membrane protein profiles (Fig. 1D), indicating the successful fusion of LP with PV without the loss of membrane proteins. The protein composition of LP and PV were determined by label-free quantification proteomics (Fig. 1E). LP exhibited almost the same expression level of typical platelet membrane proteins as PV (*e.g.*, GP Ibα, GP Ibβ, Integrin β3, CD31, XIII A, LAMTOR1, STOM, syntaxin binding protein 2, Integrin α6, and Integrin β1). On the basis of this rationale, this similar protein profile further verified the successful transfer of platelet membrane moieties onto LP. *In vitro* clot formation assay (Fig. S3 in Supporting information) revealed that after freeze-thaw, ultrasonic, and extrusion, the platelet membrane vesicle retained the physiological function of promoting coagulation and LP could promote coagulation more effectively than the platelet membrane vesicle.

The particle size and polydispersity index (PDI) of LP were measured (Table S1 in Supporting information and Fig. 2A). LP had a homogeneous size with a diameter of around 110 nm, similar to Lip, while the size of PV was above 300 nm. All these three vehicles are negatively charged (Fig. 2B). LP exhibited superior stability to Lip and PV and displayed little size change during storage at 4 °C (Fig. 2C). TEM and cryo-EM revealed that LP had a round vesicular structure and a relatively narrow size distribution (Fig. 2D and Fig. S4 in Supporting information). Based on the particle size favorable for *in vivo* circulation (Table S1) and optimal coagulation efficiency in the clot formation assay (Fig. S5 in Supporting information), LP was prepared by fusing PLT membranes with lipid membranes at the lipid:membrane protein mass ratio of 7:2. Fluorescence imaging of the blood after LP, Lip or PV injection demonstrated that the clearance of PV was very fast, but that of LP or Lip was slow (Figs. 2E and F). It was shown the LP had a similar pharmacokinetic profile to Lip, indicating that the prolonged circulation of LP was endowed by Lip (Fig. 2G and Table S2 in Supporting information). There were no differences in t1/2, MRT, and AUC between LP and Lip. The t1/2 of LP was 9.25 h, which was around 16.2 folds that of PV (Fig. 2K). Fluorescence imaging of the homogeneous solution of major organs suggested that all these three vehicles were mainly distributed in the liver, and a slight accumulation of nanovesicles was found in the heart, lung, and kidney (Figs. 2H and I). Quantitative results revealed that the accumulation of PV in the liver was 5.11 folds that of LP, and there was no difference in the accumulation in major organs between LP and Lip (Fig. 2J). These results suggested that LP had similar pharmacokinetic and biodistribution profiles to Lip.

The targeting capability of LP to vascular injury sites was investigated by *in vivo* fluorescence imaging in the mouse tail wound model. All animal protocols were approved by the Animal Ethics Committee of Fudan University. As shown in Fig. 3, regardless of the high, medium, and low doses, the LP group showed the strongest fluorescence signal at the injury vessel among the three groups at 24 h or 72 h after injection. Intriguingly, at the medium and low doses, the targeting index of LP reached above 4, which was significantly higher than that of Lip and PV at 24 h or 72 h after injection. Of note, at the high dose, the targeting index of LP increased with time and reached 20.5 at 72 h after injection, which was 8.38 folds and 13.61 folds that of Lip and PV, respectively. These results suggested that LP has a much stronger targeting to the injury site *in vivo* than Lip and PV, which could be attributed

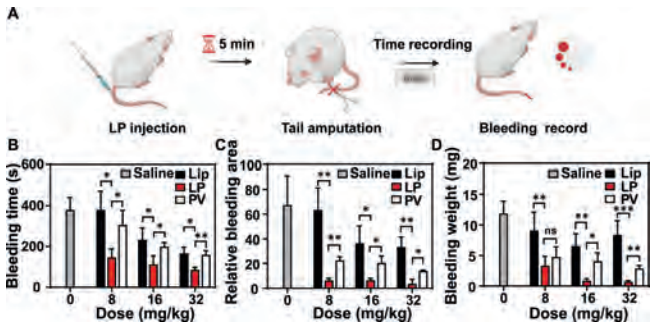

Fig. 4. *In vivo* hemostatic efficacy of LP ($n = 5$). (A) Schematic depicting the regimen of LP treatment in a mouse tail transection model. (B) Bleeding time, (C) relative bleeding area, and (D) bleeding weight of model mice after Lip, LP, and PV treatments. $^{*}P < 0.05$, $^{**}P < 0.01$, $^{***}P < 0.001$. The abbreviation "ns" indicates no significance between the two groups.

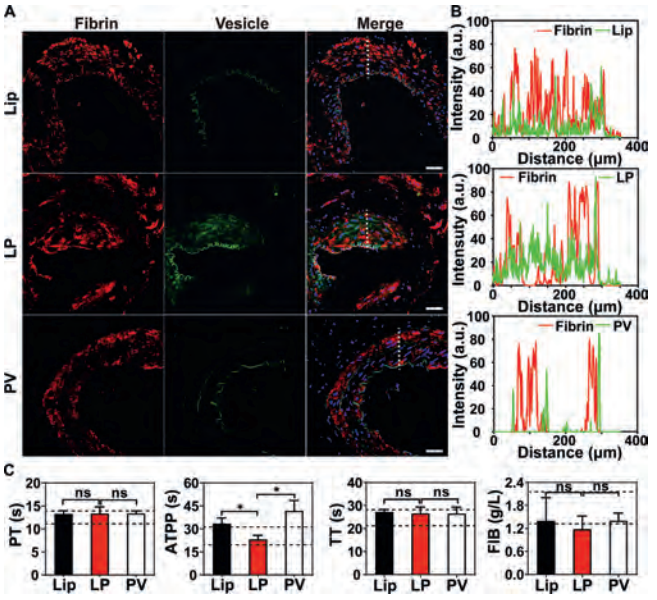

Fig. 5. (A) Representative fluorescence images of the injury vessels after LP treatment (scale bar = 100 μm) and (B) the corresponding fluorescence intensity profiles along the dotted white line crossing the representative image. Blue, cell nuclei; Green, vesicles; Red, fibrin. (C) The coagulation cascade of LP by measuring the prothrombin time (PT), activated partial thromboplastin time (APTT), and thrombin time (TT), and the fibrinogen (FIB) test ($n = 5$). $^{*}P < 0.05$. The abbreviation "ns" indicates no significance between the two groups.

to the long circulation bestowed from Lip and wound targeting capability endowed by PV.

The *in vivo* hemostatic property of LP was investigated in a mouse tail transection model (Fig. 4). As shown in Figs. 4B-D, LP treatment showed a remarkable reduction in the bleeding time, the bleeding weight, and the bleeding area at different doses compared with saline, Lip, and PV treatments. For instance, 61.4% and 52.2% reduction in the bleeding time were achieved for the LP group in comparison with that for the Lip and PV groups at the dose of 8 mg/kg, respectively. And 82.4% and 68.5% reduction in the bleeding area were achieved for the LP group in comparison with that for the Lip and PV groups at the dose of 16 mg/kg, respectively. For the bleeding weight, there was a 91.6% and 75.5% reduction for the LP group compared with that for Lip and PV treatments at the dose of 32 mg/kg, respectively. The hemostatic capability of LP increased with doses. The Lip treatment showed the weakest hemostasis at different doses among the three treatments. This is reasonable as Lip does not have any preferable binding affinity toward platelets, vWF, or collagen. PV group possessed the ability to halt the hemorrhage, substantiating that the hemostatic effect arises primarily from platelet membranes, in particular the key membrane proteins. However, due to the short lifetime of PV *in vivo*, PV had compromised hemostatic efficacy. The superior hemostatic efficacy of LP could be attributed to the long circulation bestowed from Lip and hemostatic activity endowed by PV.

The distribution of LP at the injury site was further studied to understand the hemostasis mechanism. As shown in Fig. 5A, more clots and more nanovesicles were located at the injury vessel for the LP group compared with the Lip group or the PV group. More importantly, almost all LP was located in the thrombus, and part of LP was colocalized with fibrin (Figs. 5A and B). The results suggest that LP could selectively target the damaged vessels and promote the coagulation process through binding with fibrin-like platelets. Considering that LP combing the advantages of Lip and PV demonstrated much higher hemostatic efficacy than Lip and PV, LP possesses the potential to replace clinical platelet preparations and reduce the consumption of blood products for the hemorrhage treatment.

Although LP displayed giant potential to the stoppage of bleeding, the underlying hemostasis mechanism remained ambiguous. To this end, we tested the coagulation cascade of LP. As shown in Fig. 5C, LP treatment did not significantly alter the PT, the TT, as well as the FIB but significantly reduced the APTT compared with Lip and PV treatments, indicating that LP accelerated the hemostasis mainly through promoting endogenous coagulation system to work and LP may coordinate with platelets and enhance the coagulation cascade upon the vessel injury.

No differences in the AST, ALT, BUN, and CR were found in the LP, Lip, and PV groups, and their values were in the normal range (Fig. S6A in Supporting information), indicating LP treatment at the high dose would not induce any deterioration in the kidney and liver function. As expected, LP treatment at the high dose could not cause significant changes in the WBC, RBC, HGB, and PLT level in the blood compared with Lip and PV treatments (Fig. S6B in Supporting information), suggesting that LP did not intervene in the blood cells and is biocompatible for bleeding control. As revealed in Fig. S6C (in Supporting information), no microthrombus or damages were found in any of the vital organs. These results showed that the resulting LP was biocompatible and safe for bleeding control.

In conclusion, a plateletsome was developed for hemorrhage control, and its wound targeting, hemostatic efficacy, as well as related mechanisms, were investigated. The overall outcomes indicate that this plateletsome could combine the advantages of both liposomes and platelet membrane vesicles. It had long circulation like liposomes and possessed the capability to target the injury vessels and promote blood coagulation like platelets, resulting in superior hemostatic efficacy in the murine model. Additionally, the plateletsome was biocompatible and safe. In general, this research firstly determined the hemostatic performance of plateletsome and proposed a relatively clear hemostasis mechanism, providing an alternative approach for massive hemorrhage control.

Declaration of competing interest

The authors declare that they have no known competing financial interests or personal relationships that could have appeared to influence the work reported in this paper.

Acknowledgments

We acknowledge the financial support from the National Natural Science Foundation of China (Nos. 81773283, 82070228), and

the National Key R&D Program of China (No. 2019YFC1316204). We would like to thank the National Center for Protein Science Shanghai for our Cryo-EM analysis of LP structures and membrane fusion experiment under the confocal laser scanning microscope.

Supplementary materials

Supplementary material associated with this article can be found, in the online version, at doi:10.1016/j.cclet.2021.12.091.

References

[1] X.H. Qin, K. Labuda, J. Chen, et al., Adv. Funct. Mater. 25 (2015) 6606–6617.
[2] R.K. Avery, H. Albadawi, M. Akbari, et al., Sci. Transl. Med. 8 (2016) 365ra156.
[3] B.J. Eastridge, R.L. Mabry, P. Seguin, et al., J. Trauma Acute Care Surg. 73 (6) (2012) S431–S437.
[4] D.R. King, N. Engl. J. Med. 380 (2019) 763–770.
[5] Y. Gao, A. Sarode, N. Kokoroskos, et al., Sci. Adv. 6 (2020) eaba0588.
[6] P.M. Mannucci, N. Engl. J. Med. 339 (1998) 245–253.
[7] H.T. Peng, Mil. Med. Res. 7 (2020) 1–18.
[8] C. Chen, H. Li, J. Pan, et al., Biotechnol. Lett. 37 (2015) 457–465.
[9] S.M. Moghimi, A.C. Hunter, J.C. Murray, Pharmacol. Rev. 53 (2001) 283–318.
[10] K. Ding, C. Zheng, L. Sun, et al., Chin. Chem. Lett. 31 (2020) 1168–1172.
[11] Z.M. Ruggeri, G.L. Mendolicchio, Circ. Res. 100 (2007) 1673.
[12] D. Terentes-Printzios, N. Ioakeimidis, K. Rokkas, C. Vlachopoulos, Nat. Rev. Cardiol. 19 (2022) 59–74.
[13] B. Nieswandt, D. Varga-Szabo, M. Elvers, J. Thromb. Haemost. 7 (2010) 206–209.
[14] A. Huynh, J.G. Kelton, D.M. Arnold, et al., Nature 596 (2021) 565–569.
[15] H. Tian, L. Lin, Z.J. Ba, et al., Chin. Chem. Lett. 32 (2021) 3665–3674.
[16] P. Sims, S. Rollins, T. Wiedmer, J. Biol. Chem. 264 (1989) 19228–19235.
[17] M. Olsson, P. Bruhns, W.A. Frazier, J.V. Ravetch, P.A. Oldenborg, Blood 105 (2005) 3577–3582.
[18] B. Nieswandt, S.P. Watson, Blood 102 (2003) 449–461.
[19] J.R. Fitzgerald, T.J. Foster, D. Cox, Nat. Rev. Microbiol. 4 (2006) 445.
[20] M.R. Yeaman, Cell. Mol. Life Sci. 67 (2010) 525–544.
[21] C.F. Prodger, A. Rampotas, L.J. Estcourt, S.J. Stanworth, M.F. Murphy, Semin. Hematol. 57 (2020) 92–99.
[22] C.L. Modery-Pawlowski, L.L. Tian, V. Pan, K.R. McCrae, S. Mitragotri, Biomaterials 34 (2013) 526–541.
[23] J.P. Bertram, C.A. Williams, R. Robinson, et al., Sci. Transl. Med. 1 (2009) 11ra22.
[24] N. Doshi, J.N. Orje, B. Molins, et al., Adv. Mater. 24 (2012) 3864–3869.
[25] C.L. Modery-Pawlowski, L.L. Tian, M. Ravikumar, T.L. Wong, A.S. Gupta, Biomaterials 34 (2013) 3031–3041.
[26] M. Ravikumar, C.L. Modery, T.L. Wong, A. Sen Gupta, Biomacromolecules 13 (2012) 1495–1502.
[27] F.Y. Zhu, X. Yu, S.D. Thamphiwatana, Y. Zheng, Z.Q. Pang, Acta Pharm. Sin. B 10 (2020) 2054.
[28] C.L. Modery-Pawlowski, L.L. Tian, V. Pan, et al., Biomaterials 34 (2013) 526–541.
[29] P. Laverman, O.C. Boerman, W.J. Oyen, et al., Adv. Drug Deliv. Rev. 37 (1999) 225–235.
[30] F. Gentile, C. Chiappini, D. Fine, et al., J. Biomech. 41 (2008) 2312–2318.